

Soft Matter

Accepted Manuscript

This article can be cited before page numbers have been issued, to do this please use: P. Singh, S. Misra, N. Sepay, S. Mondal, D. Ray, V. K. Aswal and J. Nanda, *Soft Matter*, 2020, DOI: 10.1039/D0SM00584C.



This is an Accepted Manuscript, which has been through the Royal Society of Chemistry peer review process and has been accepted for publication.

Accepted Manuscripts are published online shortly after acceptance, before technical editing, formatting and proof reading. Using this free service, authors can make their results available to the community, in citable form, before we publish the edited article. We will replace this Accepted Manuscript with the edited and formatted Advance Article as soon as it is available.

You can find more information about Accepted Manuscripts in the [Information for Authors](#).

Please note that technical editing may introduce minor changes to the text and/or graphics, which may alter content. The journal's standard [Terms & Conditions](#) and the [Ethical guidelines](#) still apply. In no event shall the Royal Society of Chemistry be held responsible for any errors or omissions in this Accepted Manuscript or any consequences arising from the use of any information it contains.

ARTICLE

Self-assembling behaviour of a modified aromatic amino acid in competitive medium

Received 00th January 20xx,
Accepted 00th January 20xxPijush Singh^a, Souvik Misra^a, Nayim Sepay^b, Sanjoy Mandal^c, Debes Ray^d, V. K. Aswal^d, Jayanta Nanda,^{*,a}

DOI: 10.1039/x0xx00000x

Aromatic amino acid, specifically phenylalanine (Phe), is one of the most studied building blocks in the peptide synthesis due to its importance in biology. It is reported in the literature that Phe containing peptides have a high tendency to form different self-assembled materials due to efficient aromatic-aromatic interactions. In this article, we have tuned the supramolecular interactions of phenylalanine by making it electron-deficient upon introduction of the nitro group in the ring. The presence of the nitro group has a profound influence on the self-assembly process. It has been observed that 4-nitrophenylalanine (4NP) is a highly efficient gelator than the native phenylalanine in DMSO solvent in terms of minimum gelation concentration and forms hydrogen bonding mediated crystals in water. The change of self-assembling patterns of 4NP in different solvents was studied using X-rays diffraction, UV-Vis spectroscopy, FE-SEM and other techniques. With the help of different experimental data and density functional theory (DFT), we have simulated the theoretical structure of 4NP in DMSO. The theoretical structure of 4NP in DMSO is significantly different than that of crystal in water. We have then studied the self-assembly process of 4NP in the mixed solvent of DMSO (polar aprotic) and water (polar protic). Different competitive non-covalent interactions of solvents as well as the ratio of solvent mixture guide the final self-assembly state of 4NP.

Introduction

Phenylalanine (Phe) is one of the crucial building blocks used in peptide synthesis among all the naturally occurring amino acids. Gazit and co-workers highlighted the extensive role of aromatic amino acids¹ in the amyloid fibril formation. They marked the 'Phe-Phe' residue as the core residue for the amyloid fibril formation². Later, several other research groups also described the role of diphenylalanine residue and analogues in the formation of different functional nanostructures³⁻⁸ in water, different organic and mixed solvents. With the improvement of understanding of self-assembly mechanism, scientists recently showed that simple Phe is capable of forming amyloid-like fiber in aqueous solution^{9,10}. Phe is an important amino acid as it is the precursor of the essential amino acid (e.g. tyrosine), a neurotransmitter (e.g. dopamine), several hormones (e.g. adrenaline) and skin pigment (melanin). It is found in the breast milk of mammals. In the human body, it is also accumulated

through diet. Another source of Phe is artificial sweetener¹¹ aspartame (Asp-Phe-OMe), which are frequently used in the current time. Due to metabolic disorder, the presence of an excess concentration of phenylalanine causes many diseases like phenylketonuria (PKU)¹².

In 2002, Myerson and co-workers¹³ reported thermo-reversible hydrogel (containing crystal) formation based on Phe. They termed the mixture as gel-crystal. Lloyd and co-workers recently demonstrated that simply Phe itself able to form organogel in DMSO and gel-crystal¹⁴ in water. In recent years, scientists have attempted to increase the gelation efficiency of aromatic amino acid containing known gelators^{15-20,27} by modifying the aromatic ring. This actually increases the modes of different non-covalent interactions namely π - π interactions, hydrogen bonding, hydrophobic and electrostatic interactions between the gelator molecules and results in the enhanced gelation properties. Several chemical modifications of the aromatic ring were attempted to improve the mode of interactions. In this regard, pioneer works were done by Nilsson and co-workers^{17,19}. Ring substituted phenylalanine derivatives of 9-fluorenylmethoxycarbonyl [Fmoc-Phe(X)-OH] exhibited efficient hydrogelation compared to the simple Fmoc-Phe-OH^{21,22}. Their works suggested that gelation efficiency depends upon the nature and number of halogen group/s and their position in the aromatic ring^{19,20}. Metrangolo and co-workers highlighted the role of halogen bonding^{5,18,23,24} interactions in the para-substituted halogen derivatives of Fmoc-Phe-OH¹⁸ and short amyloid peptide²³. Lloyd recently showed how viscoelastic property and solid-state packing change on the introduction of

^a Department of Chemistry, Indian Institute of Engineering Science and Technology, Shibpur, P.O.- Botanic Garden, Howrah-711103, West Bengal, India. Email: jayanta2017@chem.iests.ac.in & drjayantananda16@gmail.com

^b Department of Chemistry, Jadavpur University, Jadavpur, Kolkata-700032

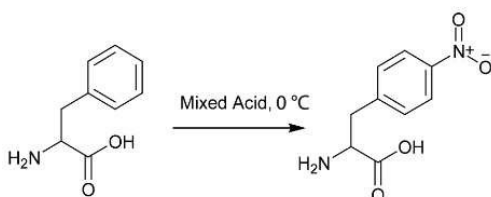
^c Polymer Science Unit, Indian association for the Cultivation of Science, Jadavpur, Kolkata-700032

^d Solid State Physics Division, Bhabha Atomic Research Centre Trombay, Mumbai, 400085 India

† Footnotes relating to the title and/or authors should appear here.

Electronic Supplementary Information (ESI) available: [details of any supplementary information available should be included here]. See DOI: 10.1039/x0xx00000x

halogen group in the ring of phenylalanine²⁵. So, the introduction of different substituents in the aromatic ring of amino acid enhanced the gelation efficiency significantly^{5,18,20,25-27}.



Scheme 1. Synthetic scheme of 4-nitrophenylalanine (4NP). Reagents and condition: mixed acid (Conc. HNO₃ and Conc. H₂SO₄) at 0 °C.

Inspired by these works, we have introduced one simple functionality (nitro group) in the aromatic ring of phenylalanine to evaluate the effect of ring substitution on self-assembly. Regular nitration method was used for the incorporation of the nitro group at the cold condition. Nitro group is incorporated in the para position of the phenyl ring of Phe. Here, presence of nitro group makes the aromatic ring electron-deficient. According to our strategy, we are interested in the self-assembly of electron-deficient 4-nitrophenylalanine (4NP) in different organic and aqueous solution. In this work, we have serendipitously found that 4NP can form efficient organogel in dimethyl sulphoxide (DMSO). It is already known that 4NP forms crystal in water²⁸. DMSO and water are miscible solvents. So, it will be interesting to study the self-assembly property of 4NP in water, DMSO and their mixtures. In pure DMSO solvent, it forms reddish coloured organogel. Nanoscale morphology using FE-SEM and SANS studies suggested the formation of nanofibers in DMSO. Crystallization and gelation are the nucleation process of the molecule which lead to the emerging properties of materials²⁹⁻⁴⁵. In the gel, molecules undergo self-assembly to form unidirectional fiber, whereas in crystal highly directional, three-dimensional arrangements occur. A recent report²⁹ suggests that the nucleation process in gelation is kinetically favoured however crystallization is thermodynamically favoured process. In this work, we have studied the self-assembly of 4NP in two pure solvents and in their mixture. It is observed that the ratio of the solvent dictates the possible final self-assembly state. Competition between charge-transfer and hydrogen bonding mediated interactions were studied in the mixed solvent using several techniques including UV-Vis, FE-SEM, rheology and XRD analysis.

Results and Discussion

Gelator compound was synthesized by the nitration²⁸ of phenylalanine at 0 °C (Scheme 1). Compounds were purified by the crystallization from water. Faint yellow coloured crystalline 4NP was used further for all the experiments.

Self-assembly in DMSO

For characterization of newly synthesized material, NMR technique was used. 4NP crystals are not readily soluble in DMSO-d₆ solvent and under heating condition, 4NP was

dissolved into solution. Serendipitously, we noticed that 4NP forms beautiful reddish coloured transparent organogel within the NMR tube upon cooling at ambient temperature. The gel formation of 4NP in regular DMSO solvent was further checked in a glass vial by 'inverted test-tube' technique. One interesting observation is that 4NP crystal is almost colourless, but when it was dissolved in DMSO, the solution turns into a reddish colour. The gelation efficiency of 4NP in DMSO was measured and its gelation efficiency is better than native Phe residue¹⁴. The measured minimum gelation concentration (MGC) is 19.2 mM. It is calculated that 4NP forms almost 2.6 times efficient gel in DMSO than its native form¹⁴ in terms of MGC. This observation suggested that slight modification of the structure leads to better gelator in DMSO. Organogel exhibits thermo-reversible nature. The gel-sol transition temperature i.e. gel melting temperature (T_{gel}) was measured at different concentrations (mM) and plotted as Fig. 1b. T_{gel} values of DMSO-gel increase with increasing concentration of 4NP⁴⁶.

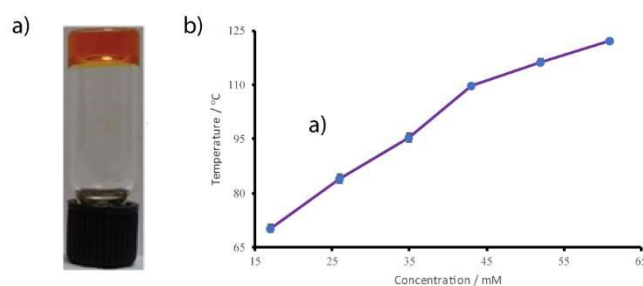


Fig. 1 a) Image of 4NP-organogel in an inverted glass vial and b) concentration-dependent thermal stability of 4NP organogel in DMSO.

Variable temperature NMR (VT-NMR) experiment was done to know the effect of temperature on the gelation. The fine changes due to different supramolecular interactions are usually reflected in an NMR experiment. Here, a temperature-dependent ¹H NMR study was carried out to understand the role of different non-covalent interactions present in the organogel state. It is obvious that with the increase of temperature, the interactions of the gelator-gelator and gelator-solvent molecules will be influenced. During VT-NMR study, the temperature was increased from 40 to 90 °C (ESI, Fig. S3). It is observed that with the increase of temperature aromatic protons are down-fielded^{47,48} i.e. the aromatic-aromatic interactions of 4NP were diminished which leads to the gel to sol transition. So, aromatic-aromatic interactions play a pivotal role in gel formation.

SANS study

4NP gel material was studied using small-angle neutron scattering (SANS) experiment. Fig. 2 shows the scattering profile of 4NP at 30 °C. In the low- Q region of the data, the scattering intensity decreases in almost a straight line as $1/Q^2$ and it indicates the cross-section of bundle-like structures in these systems. The absence of lower cut-offs in the data indicates that the length of these bundles could be much larger than what can be determined from the present Q_{min} and therefore the length was kept fixed higher than to a value $2\pi/Q_{min}$, i.e., ~ 400 Å.

These bundles of the fiber-like structure have been characterized by the cross-sectional radius or thickness as the measurement of the length is limited by the Q_{\min} of the SANS instrument. The average thickness of the bundle of the fiber-like structure has been found to be 28 Å.

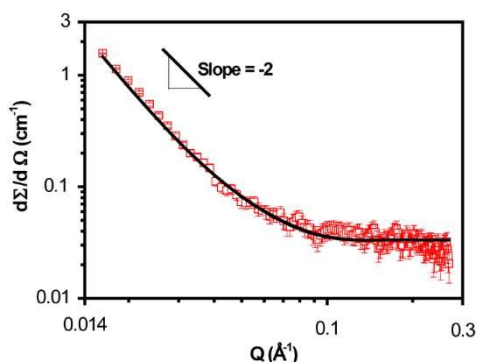


Fig. 2. SANS scattering profile for 4NP-DMSO gel measured at 30 °C.

Self-assembly in Mixed solvents (DMSO and Water)

During the gel formations, apart from gelator-gelator interactions, gelator-solvent interactions play a crucial role. To understand the solvent-gelator interactions in the gel state, as well as, competitions among different solvents for a gelator in the gel state, another solvent system (water) was introduced in DMSO solution of 4NP. DMSO is one of the highly polar solvents and highly miscible in water. Our studied gelator 4NP is also soluble in water and forms crystal in it²⁸. We studied the self-assembly of 4NP in the mixed solvent system (varied ratios of DMSO and water) at a fixed concentration of 4NP. In the solvent mixture, two solvents will interact with 4NP using different non-covalent interactions and try to modulate the final self-assembly state as like their self-assembly in pure solvent.

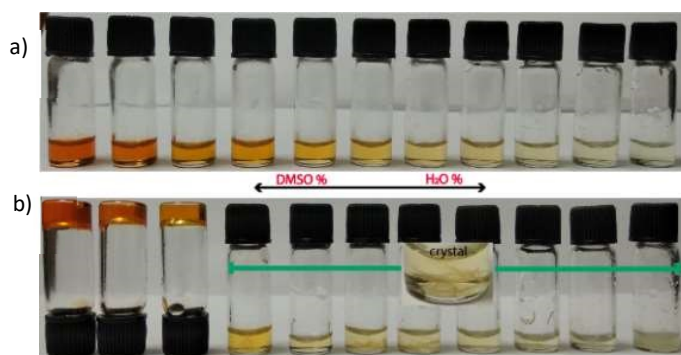


Fig. 3 Optical images of glass vials containing 4NP in different DMSO-water mixtures: a) under the hot condition and b) after equilibration of 24 hrs. The extreme left vial contained 100 % DMSO and the water content was increased 10 % in each next vial.

A set of mixed solvent (DMSO+water) was prepared by increasing the percentage of the water. In Fig. 3a, only pure DMSO was taken in extreme left vial (100 % DMSO), after that, in each vial water content was increased 10 % till the extreme right vial where only 100 % water was taken. Then, crystalline

4NP (1.0 mg) was added in different vials having 0.25 ml solvent. The resulting solutions were heated until the clear solutions were obtained. All these solutions were kept at room temperature for equilibration. Within a few minutes, a red-coloured gel was formed in 100% DMSO (extreme left vial in Fig. 3b). With the increase of the water percentage in the solution, the reddish colour was diminished and turned to form an almost colourless (faint) solution in pure water (extreme right). Around 30 minutes, needle-shaped crystal formation took place from the vial with 100 % water (extreme right vial in Fig. 3b). Within one hour, it was observed that solutions (% of DMSO 90 and 80) were transformed into gel *i.e.* 4NP can form self-supported gel even in presence of 20 % water. Longer time duration indicates that the presence of water slowed down the gel formation kinetics. But, the rest of the vials remained as a solution. An interesting observation was noticed after overnight equilibration. The solutions present in the rest of the vials did not form gel rather needle-shaped crystals of 4NP in the bottom of the glass vials.

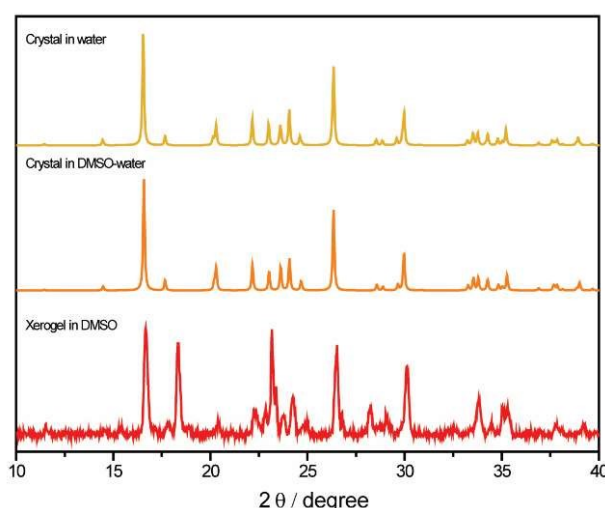


Fig. 4 PXRD patterns of xerogel of 4NP in DMSO (red) and simulated XRD pattern of 4NP grown in DMSO-water mixture (orange) and water (yellow).

In the presence of water (>20%), non-covalent interactions of water with 4NP molecules dominated in the solutions and water facilitated the formation of thermodynamically stable crystal in the rest of the solutions. We studied the powder XRD pattern of the xerogel (from DMSO) and the simulated XRD pattern of crystals grown from pure water and DMSO-water mixture (ratio= 50:50) in Fig. 4. It is clear that packing pattern is same for the crystals which are grown in water or water-DMSO medium. The XRD pattern of 4NP in DMSO is quite different from the crystal. During this study, we have varied the gelator concentration and noticed that increased in concentration of 4NP can gelyfy the mixed solvent even above 20 % of water content.

Hansen Parameter

It is already noticed that gel and crystal formation of 4NP was dictated by the solvent ratio. Recently, some researchers have applied the 'Hansen solubility parameter' for understanding gel formation/crystallization ability in a similar type of solvents by

accounting three types of interactions: polar (δ_p), van der Waals (δ_d) and hydrogen bonding (δ_h) interactions of a solvent. By balancing these three interactions, a molecule can form a gel or remains soluble or insoluble in a particular solvent^{44,49}. Here, the physical state of 4NP in DMSO, water, and mixture of DMSO-water was compared using the Hansen solubility parameter (δ_p , δ_d , δ_h). For the DMSO-water mixture system, the Hansen solubility parameter was calculated by assuming a linear relationship⁴⁹

$$\delta_{mixture} = x_{water} \times \delta_{water} + (1 - x_{water})$$

where x_{water} is the fraction of water in the mixture (v/v). For DMSO and water, van der Waals interaction (δ_d) values are respectively 18.4 and 15.5 and also polar interaction (δ_p) values are 16.4 and 16.2 respectively. These two interaction values are quite similar for DMSO and water. But the hydrogen bonding parameter of DMSO and water are 10.2 and 42.4 respectively which has a huge difference. In DMSO, 4NP molecules self-assemble by balancing three solubility parameters. During the addition of water in the DMSO medium, hydrogen bonding propensity of resulting solvent was increased linearly. Therefore, hydrogen bonding (δ_h) interactions with 4NP are getting more preferences and guides the overall system towards crystallization (ESI, Fig. S4). Up to 20% of the water in the DMSO, 4NP can retain its gel behaviour and after that crystallization of 4NP occurs.

UV-Vis spectroscopy study

The interesting colouration of 4NP in solution and gel state (Fig.3) makes us curious to know the reason behind it. For this purpose, we studied the UV-Vis absorption spectra of 4NP in water, DMSO and mixed solvents. We prepared solutions of 4NP (50 μ M) in different mixed solvents and solutions were equilibrated for 30 minute prior to the UV-vis spectroscopic study. In water, a characteristic peak at 274 nm was noticed, which is due to the π - π^* transition of nitroaromatic functionality present in 4NP. In DMSO, apart from a peak at 300 nm, a characteristic peak at the longer visible wavelength (477 nm) was observed. The colouration in DMSO is due to the interactions of 4NP with DMSO. This is a charge-transfer (CT) interactions⁵⁰⁻⁵² between electron-rich DMSO with electron-deficient 4-nitro phenylalanine. This intense visible region peak was diminished, upon addition of water into the DMSO solution. It is assumed that DMSO solvent and 4NP are participating to form charge-transfer complex, which is diminished in presence of water having high hydrogen bonding capability.⁵³ Competition between two solvents for 4NP is monitored by UV-Vis spectroscopy in a mixed solvent (Fig. 5a). Upon changing the solvent system from 100% DMSO to 100% water, the charge-transfer band is diminished. The decrease of the absorbance value at 477 nm with the % of water in the mixture was plotted in Fig. 5b. It is clear from the plot that the extent of CT interaction was drastically decreased upon addition of water. Moreover, the π - π^* transition band (\sim 300 nm) was shifted towards shorter wavelength (Fig. 5a), i.e. blue shift occurs. This blue shift is possibly due to the continuous breaking of extended aromatic-aromatic interactions of the 4NP in DMSO. So, all these observations clearly indicate that there is a strong

competition between DMSO (through CT interaction) and water (through hydrogen bonding interaction) for 4NP in mixed solvent. In presence of water (> 20 %), hydrogen bonding interactions of 4NP-water overcomes the charge transfer interactions of 4NP-DMSO and favours the formation of the crystal in the mixed solvents.

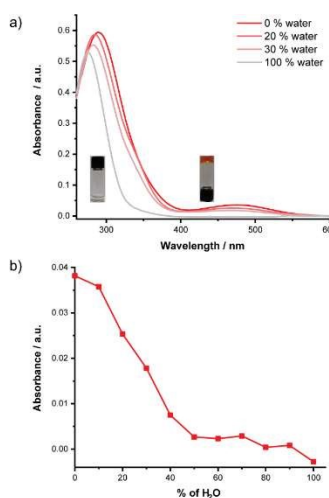


Fig. 5. a) UV-Vis spectra of 4NP (50 μ M) in different solvents. The composition of the solvents is given in the figure legends. b) The variation of charge-transfer band (477 nm) intensity with the percentages (%) of water in the mixed solvents.

Morphology of Gel

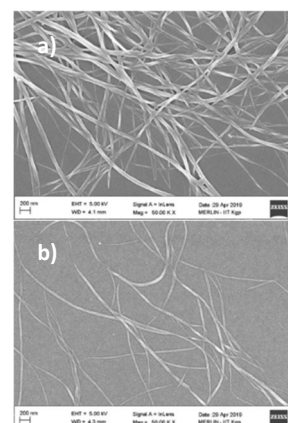


Fig. 6 FE-SEM micrographs of 4NP in a) 100% DMSO and b) 20 % water in DMSO-water mixture. Scale bar is 200 nm.

For understanding the self-assembly behaviour and nanoscale morphology of 4NP in mixed solvents, field emission scanning electron microscopy (FE-SEM) was used. FE-SEM image of DMSO-gel is shown in Fig. 6a. 4NP forms dense, cross-linked nanofibers in DMSO. These fibers are several micrometer long and the average fiber-width is around 60 nm (ESI, Fig. S5a). The effect of water on the self-assembly process in the mixed solvent (20 % water in DMSO) was also investigated by FE-SEM study. It is observed from the image (Fig. 6b) that the density of fiber decreased noticeably and the average fiber-width is around 40 nm (ESI, Fig. S5b). SEM study demonstrates that 4NP molecules are self-associated in DMSO to form kinetically stable 1D nanofibers which are cross-linked to each other and trap

DMSO solvent to form a gel. In addition to water, the self-assembly process of 4NP in DMSO was affected by the competing hydrogen bonding interactions of 4NP and water. This results in the less dense, thinner fiber formation.

Rheology of gel

The strength of gels, prepared in different solvents, were examined with the help of a rheometer. Viscoelastic gel materials exhibit storage energy as well as loss energy. The higher value of storage modulus (G') than loss modulus (G'') at constant frequency represents the gel behaviour^{30,54} At critical stress value, storage modulus (G') and loss modulus (G'') crossed each other and gel becomes sol. Here, to evaluate the addition of water on the self-assembly process of 4NP in DMSO, oscillatory stress sweep experiments of 4NP-gel were performed in two conditions by preparing gels in 100% and 80 % DMSO solvent at a fixed concentration of 4NP (0.75 % w/v). From the Fig. 7, it is observed that in the linear viscoelastic region (LVR), the storage modulus (G') values are higher than loss modulus (G'') in both solvent system^{55,56}. The storage modulus value in the LVR region of 4NP gel (in 100% DMSO) is comparable with the native L-phenylalanine gel in DMSO¹⁴ reported earlier. The measured critical stress value in DMSO is 201 Pa, while in 20 % water in DMSO, critical stress value is 171 Pa. These results suggest that with increasing of water fraction in the solvent mixture, the gel loses its strength.

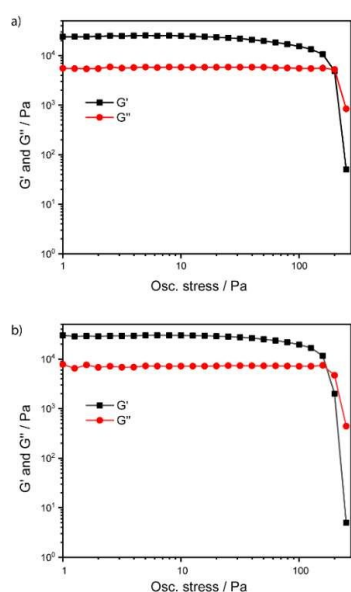


Fig. 7 Oscillatory stress sweep experiment of 4NP-gel in a) 100% DMSO and b) 80% DMSO in DMSO-water mixture respectively. The concentration of gelator was kept 0.75 % (w/v).

The three-dimensional arrangement of 4NP in the crystal was characterized by single-crystal X-ray technique. Needle shaped crystal was grown in water by slow evaporation. A monohydrated 4-nitrophenylalanine crystalized in the monoclinic space group $P12_11$. The asymmetric unit of 4NP is consisting of one 4NP molecule in zwitterion form and one water molecule. We have also compared the crystal structure 4NP with the native Phe which crystalized in monoclinic space group $P2_1$.⁵⁹ We found that 4NP have sufficient similarity and

dissimilarity with the crystal behaviour of Phe. Interestingly, the b axes of 4NP unit cell ($b = 5.293(4)$) is 176 times shorter than that of Phe ($b = 30.8020(17)$) [ESI, Table-S1]. In solid-state, three 4NP molecules are interlocked by a single H₂O molecule along a and b axes (Fig. 8b & ESI Fig. S6-S7). The intermolecular H-bonding distances for N9-H9B...O11, O11-H11A...O7 and O11-H11B...O8 are 1.885 Å, 1.883 Å and 2.020 Å respectively. Such hydrogen bonding interaction is absent in Phe since it does not contain any water of crystallisation. In the lattice, a network arrangement of 4NP creates one hydrophilic and one hydrophobic zone due to their tail-tail and head-head interactions. In the hydrophilic zone, the deprotonated carboxylic group and protonated amine group were connected via electrostatic attraction (with distance 2.909 Å) and stabilized via water-mediated H-bonding interaction. This type of hydrophilic and hydrophobic zones are also observed in the crystal structure of Phe. Along c axis, hydrogen bonding distance of ring-hydrogen (H4) of 4NP with oxygen (O9) of the nitro group of another 4NP is 2.720 Å. This intermolecular strong hydrogen bonding interaction helps to form head to head arrangement of the aromatic ring along c axis. Here, additional C-H... π interaction is identified along b axis. The interaction between β -H (H12A) and phenyl ring of another 4NP molecule along b axis with distances 2.823 Å, made two aromatic ring parallel.

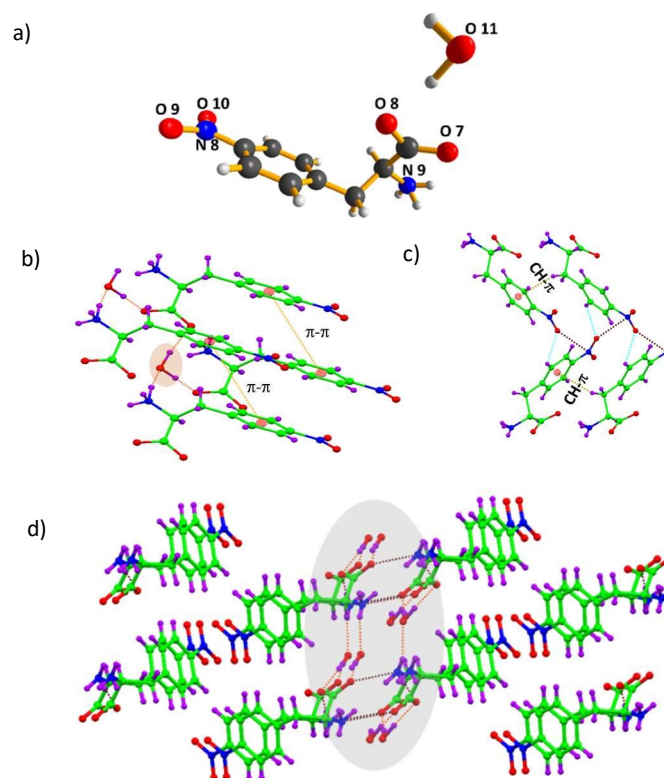


Fig. 8 a) ORTEP diagram of 4NP. Different non-covalent interactions present in the crystals: b) water-mediated hydrogen-bonding interactions and aromatic-aromatic interactions and c) H-bonding interaction and CH- π interactions. d) Formation of the hydrophilic zone due to ionic interactions of COO⁻ and NH₃⁺ of two adjacent 4NP molecules in the higher-order packing.

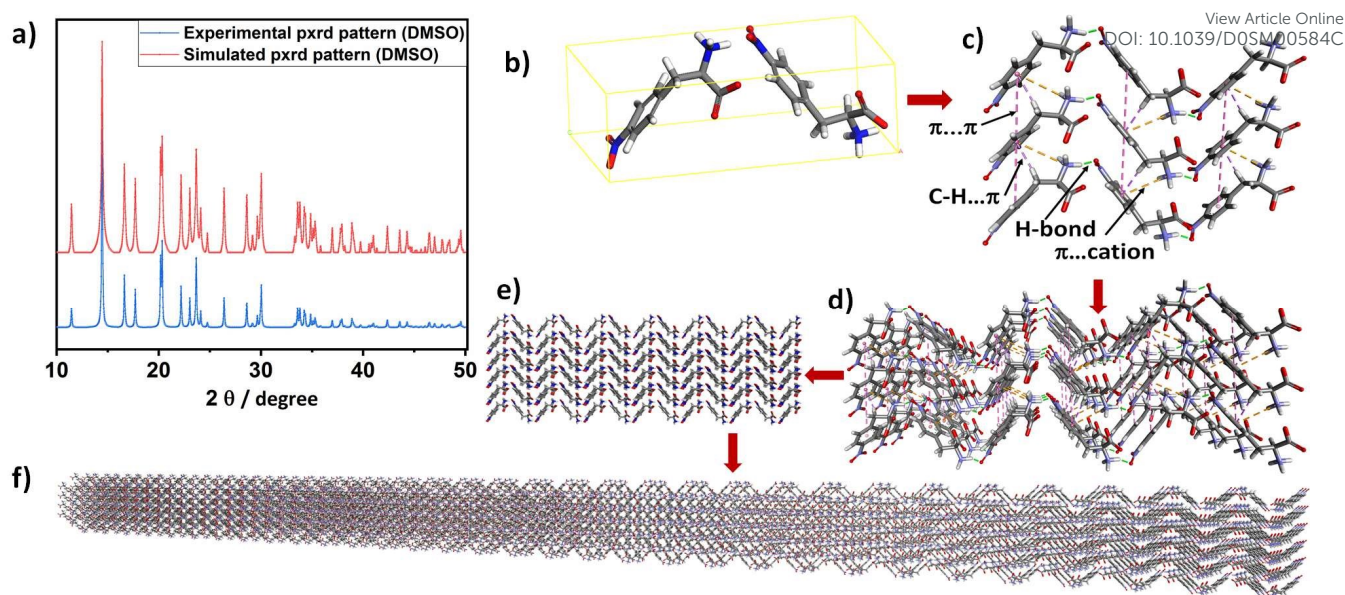


Fig. 9: a) Fitting of simulated and experimental powder X-ray crystallographic patterns of 4NP packed in DMSO; b) head-to-tail arrangement of 4NP in unit cell of nanofiber; c) intermolecular interactions in 4NP molecules; d) arrangements of the 4NP molecules in three dimension with the help of supramolecular interactions; e) higher order packing of 4NP; f) formation of nanofibers through self-assembly of 4NP.

Incorporation of the nitro group introduces new intermolecular H-bonding interactions which help to arrange the molecules in a zig-zag manner along *c* axis. However, in the Phe crystal, this type of zig-zag formation is grown along the *b* axis.

Computational Simulations

Understanding the change of arrangements of 4NP molecules inside the crystal which form the nanofibers in less polar solvent (water to DMSO) is important to unravel the structure-photophysical relationship of 4NP. Here, we have assumed that same number of molecules present in a unit cell creating the nanofibers in DMSO, like its single-crystal formed in water. We have changed the molecular orientation randomly with different crystal symmetry and calculated the powder x-ray pattern of each orientation to fit with the pattern of nanofibers found experimentally. During this process, the cell parameters obtained from single-crystal X-ray crystallography have been used. It was found that the powder X-ray pattern of 4NP packed with *Pc* space group fits very well with the experimental pattern (Fig. 9a) and the unit cell is shown in Fig. 9b. Computationally generated system contains a glide plane perpendicular to $[0, 1, 0]$ plane with glide component $[0, 0, \frac{1}{2}]$, where the single crystal system has 2-fold screw axis with direction $[0, 1, 0]$ at $0, y, 0$ with screw component $[0, \frac{1}{2}, 0]$.

The molecular arrangements are very helpful to realize the nanofiber formation mechanism with the help of intermolecular weak interactions. In presence of water, the zwitterionic and highly polar 4NP molecules trend to interact more with water through hydrogen bonding rather than its intermolecular hydrogen bonding to form nanofiber. This solvent interruption

in intermolecular hydrogen bonding is responsible for the higher solubility as well as the non-gelation tendency of 4NP in water. The molecule crystallizes with water form hydrogen bond with the acid group inside the unit cell and forms a hydrophilic zone. In the presence of less polar and aprotic solvent DMSO, the 4NP molecules preferred to form less-polar head-to-tail arrangement (Fig. 9b). The aprotic nature of solvent helps to form strong hydrogen bonding (1.43 Å) between ammonium and nitro groups and gives a stable zig-zag chain (Fig. 9c). Such multiple chains can stack parallel way with each other through different supramolecular interactions (Fig. 9c). Here, π - π stacking of nitrobenzenes ring, C-H... π and π -cation interactions are in the behind of the association of large number of molecules in an organized way (Fig. 9c). The three-dimensional repetition of such arrangements in high-order packing is able to produce a nanofiber like structures (Fig. 9d-f). These theoretical results corroborate the experimental observations satisfactorily.

The studies have been extended to TD-DFT for finding the reason of the solvatochromic behaviour of 4NP during self-assembly in DMSO. The calculations show that the molecular arrangement presented in Fig. 9b absorb at λ_{\max} 490 nm (experimental value, $\lambda_{\max} = 477$ nm; Fig. 4a) with the 0.068 oscillation strength (Fig. S9). The transitions from HOMO-2 to LUMO (26%), HOMO-1 to LUMO (62%) and HOMO to LUMO (5%) contribute mainly for the absorption (Fig. S9). The energy difference for HOMO-1 to LUMO energy levels is 3.1 eV. The detail of the studies are given in ESI. The closely fitting of PXRD and λ_{\max} value obtained from theory with the corresponding

experimental data validate the assumptions and support the mechanism of formation nanofiber in DMSO.

Hirshfeld analysis

Hirshfeld analysis⁵⁷ was used to understand the role of different mode of interactions in the lattice packing of the 4NP molecule, which stabilize the three-dimensional arrangement. In the crystal packing, the Hirshfeld surfaces express the volume occupied by a monomeric molecule in the lattice by dividing crystal electron density into a molecular fragment⁵⁸. The Hirshfeld surfaces of the molecule is mapped by d_{norm} (normalized for the atom size) function. The intense colour on the surfaces represents the different type of intermolecular interaction zone, which present in the molecule. Here, the intense red colour zones signified the strong hydrogen bonding interaction site which brings the molecule in the close vicinity. Here, the red zones represent the hydrogen bonding sites (COO and NH_3^+ group) which form hydrogen bonds with a water molecule (Fig. 10 a). Hydrogen bonding interactions present in the crystal is shown in Fig. 10b via two-dimensional fingerprint plot. The contribution of donor-acceptor close contact is plotted in the fingerprint plot by calculating the nearest interior (d_i) and exterior (d_e) nuclei distances to the Hirshfeld surfaces. The close contact contribution of O...H interactions are visually observed in the 2D fingerprint plot (Fig. 10b). For 4NP, in the fingerprint plot, the spikes represent the maximum close contact contribution of strong O...H interactions. It can be concluded from the Hirshfeld surfaces that the arrangement of the 4NP molecule is specially stabilized by hydrogen bonding interaction (46.3 %) via a water molecule.

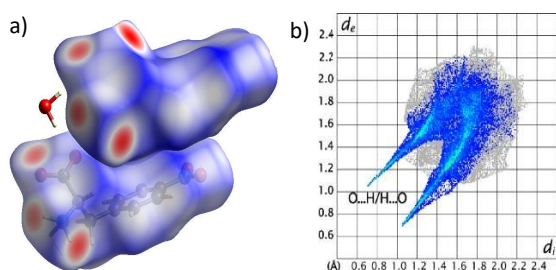


Fig. 10 a) Hirshfeld surface of the 4NP mapped over d_{norm} , b) Two-dimensional fingerprint plots for 4NP and relative contributions of the atom pairs (O...H) to the Hirshfeld surface.

Conclusions

In this article, we have successfully demonstrated that the incorporation of new functionality in the ring of aromatic amino acid residue modifies the supramolecular interactions. Here, we are first time reporting that the presence of the nitro group in the phenylalanine (4NP) makes it a better gelator than the native form in DMSO solvent in term of gelation efficiency. In DMSO, a reddish colour gel is obtained due to charge transfer complex formation. The gel materials are extensively characterised using different techniques including FE-SEM, XRD and rheology. In water, the same modified aromatic amino acid

also forms crystal. In the presence of a nitro group, several additional non-covalent interactions take part to form a three-dimensional structure in solid-state which are absent in the crystal structure of simple phenylalanine⁵⁹. Out of them, water molecule-mediated hydrogen bonding interactions with three 4NP molecules and CH- π interaction are of special interest. We have also studied the self-assembly of 4NP in the mixed solvent of DMSO and water, which is an interesting study indeed. Solvent molecules are interacted with the 4NP using different non-covalent interactions like hydrogen bonding interaction (water) and charge-transfer interaction (DMSO). We find that final self-assembly state in mixed solvent is dictated by the solvent composition.

Experimental Section

Synthesis of 4-Nitro-Phenylalanine (4NP)

4-Nitrophenylalanine was synthesized using the procedure reported in the literature^{28, 61}. 1.65 g (10 mmol) of L-phenylalanine was taken in a round bottom flask along with 2 mL conc. H_2SO_4 and mixed properly by a stirrer at the ice-cold condition. After 15 min, mixed acid (0.7 ml conc. H_2SO_4 and 0.7 ml conc. HNO_3) was added drop-wise with continuous stirring for 1 hr. Then, the solution was allowed to stir at room temperature for 4 hrs. The reaction mixture was poured into 100 ml ice-cold water with continuous stirring. The resulting solution was basified with liquor ammonia. The volume of the resulting solution was reduced until the precipitation appeared. The faint yellow coloured solid mass was obtained and recrystallized in water. Shining needle-shaped crystal was grown in the water medium.

Materials and Methods

L-phenylalanine was purchased from SRL chemical, India. Conc. H_2SO_4 , conc. HNO_3 and liquor ammonia were purchased from Spectrochem, India. Distilled water was used throughout the experiment. All analytical grade solvents were purchased from Finar, India and distilled prior to use.

NMR: ^1H NMR study of 4NP was conducted using BRUKER 300 MHz NMR spectrometer. Compound 4NP was dissolving in DMSO-d_6 at 0.6 % (w/v) by heating. With the gel materials, the temperature-dependent ^1H NMR study was conducted at 30 to 95 °C range by raising the temperature. Before every scan at a different temperature, the system allowed to equilibrate for 10 min.

HRMS: For molecular weight determination, ESI- MS^+ spectra were recorded on a QTOF Micro YA263 mass spectrometer. The compound 4NP was taken with acetonitrile solvent.

Gel melting temperature measurement: The gel-melting temperature was measured using a digital oil-bath. Gel was prepared in a screw cap glass vial (capacity 1mL, diameter 10 mm) and the melting temperature was noted using the 'inverted test-tube method'. Temperature of water-bath was increased 1 °C/min. For each concentration, three readings were taken and average gel-melting temperature was plotted against the corresponding concentration.

SANS: Small-angle neutron scattering experiments were performed at the SANS diffractometer at Guide Tube Laboratory, Dhruva Reactor, Bhabha Atomic Research Centre, Mumbai, India⁶⁰. In SANS, one measures the coherent differential scattering cross-section ($d\Sigma/d\Omega$) per unit volume as a function of wave vector transfer $Q (= 4\pi \sin\theta/\lambda$, where λ is the wavelength of the incident neutrons and 2θ is the scattering angle). The mean wavelength of the monochromatized beam from the neutron velocity selector is 5.2 Å with a spread of $\Delta\lambda/\lambda \sim 15\%$. The angular distribution of neutrons scattered by the sample is recorded using a 1 m long one-dimensional He3 position-sensitive detector. The instrument covers a Q-range of 0.015–0.30 Å⁻¹. The data have been analyzed by comparing the scattering from different models to the experimental data.

UV-Vis: UV-visible spectra were recorded on a Shimadzu 2401 PC UV-vis spectrophotometer. The samples were prepared in 100% DMSO, 100% water and mixed solvents. The concentration of 4NP was 50 µM in each solvents. During measurement of each different 4NP solution, spectrometer was calibrated using that particular solvent system.

Xerogel Preparation: First, gel was prepared by dissolving 4NP-crystals in DMSO under heating condition. The resulting solution was cooled at room temperature to get the organogel. Then, solvent was removed from this gel by connecting with high vacuum pump in a vacuum desiccator for two days to get xerogel.

PXRD: For the determination of powder X-ray diffraction (PXRD) patterns of the xerogel, Bruker D8 Discover instrument using Cu-K α ($\lambda = 1.5406$ Å) radiation was conducted.

Field Emission Scanning Electron Microscope (FESEM): By using a ZEISS SIGMA FE-SEM instrument, Field-emission scanning electron microscopy (FE-SEM) experiment was performed. For the sample preparation, 4NP was taken in different glass vial with 100 % DMSO and 20% water in DMSO at 0.6 % (w/v) concentration. Then, using heating cooling technique, gels were prepared. The freshly prepared gel was placed on the clean glass coverslip. This organogel was first dried in air. Before the gold coating, samples were placed in high vacuum for 2 days.

Fiber width measurement: The width of the nanofiber, which was obtained by the FESEM study was measured by the help of the Image-J software.

Oscillatory Rheological Measurements: The mechanical properties of the organogel of 4NP were investigated by an advanced rheometer (AR 2000, TA Instruments, USA) using cone plate geometry on a Peltier plat at 25 °C temperature. The diameter of the plate was 40 mm and the angle was 4° with a plate gap of 121 µm. 2 mL organogel was transferred on the rheometer plate by using the spatula. In an oscillatory stress sweep experiment, storage modulus (G') and loss modulus (G'') were measured.

Single Crystal X-ray Diffraction: X-ray quality crystal of 4NP was grown in H₂O medium by the slow evaporation method. Good quality of single crystal was used for X-ray data collection. On the tip of the glass fiber, a single crystal of 4NP was mounted by using commercially available adhesive. Using Bruker APEX III diffractometer with monochromatic Mo-K α radiation ($\lambda = 0.71073$ Å) and the X-ray data were collected at room

temperature (293 K). The collected X-ray data were integrated using SAINT-NT software package and with the help of the SADABS program, absorption correction was made. The structure was reduced by the help of the SHELX 2013 program⁵⁶, and refined by full-matrix least-squares on F2. For all non-hydrogen atoms, anisotropic thermal displacement parameter was employed. The X-ray structure refinement parameters and details of the X-ray structure were summarised in tabular form.

Computational Simulations: The structure of 4NP was optimized in solid-state with the help of DMol3 using LDA-PWC functional and DND basis set with 3.5 basis file. These results were visualized by Discovery studio. TD-DFT calculations were performed by Gaussian 09W with D.0158 revisions at B3LYP level of theory through 6-31g basis set.

Hirshfeld Analysis: The electrostatic surface of the compound 4NP, designed by d_{norm} (Normalized for the atom size) function using CrystalExplorer software. Crystallographic Information File (cif) of compound 4NP was used in Hirshfeld surface analysis.

Conflicts of interest

There are no conflicts to declare.

Acknowledgements

JN gratefully acknowledges DST-INSPIRE Faculty Grant (IFA16-CH246) and Department of Chemistry, IEST-Shibpur for financial assistance. We are thankful to Prof. A. K. Nandi for rheological study. JN is sincerely thankful to SAIF-IEST for single crystal X-rays diffraction study.

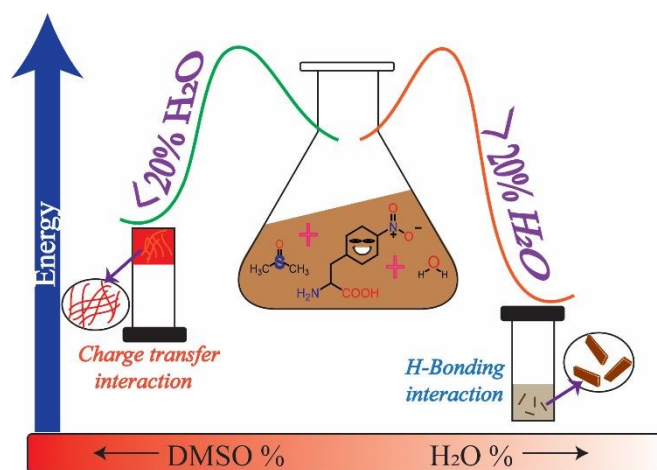
Notes and references

† Footnotes relating to the main text should appear here. These might include comments relevant to but not central to the matter under discussion, limited experimental and spectral data, and crystallographic data.

- 1 E. GAZIT, FASEB J., 2002, 16, 77-83.
- 2 M. Reches and E. Gazit, *Science*, 2003, **300**, 625-627.
- 3 S. Marchesan, A. Vargiu and K. Styan, *Molecules*, 2015, **20**, 19658.
- 4 D. Datta, O. Tiwari and K. N. Ganesh, *Nanoscale*, 2018, **10**, 3212-3224.
- 5 A. Pizzi, V. Dichiarante, G. Terraneo and P. Metrangolo, *Peptide Sci.*, 2018, **110**, e23088.
- 6 R. Xing, C. Yuan, S. Li, J. Song, J. Li and X. Yan, *Angw. Chem. Int. Ed.*, 2018, **57**, 1537-1542.
- 7 X. Yan, P. Zhu and J. Li, *Chem. Soc. Rev.*, 2010, **39**, 1877-1890.
- 8 T. Das, M. Häring, D. Haldar and D. Díaz Díaz, *Biomater. Sci.*, 2018, **6**, 38-59.
- 9 S. Perween, B. Chandanshive, H. C. Kotamarthi and D. Khushalani, *Soft Matter*, 2013, **9**, 10141-10145.
- 10 V. Singh, R. K. Rai, A. Arora, N. Sinha and A. K. Thakur, *Sci. Rep.*, 2014, **4**, 3875.
- 11 B. G. Anand, K. P. Prajapati, K. Dubey, N. Ahamad, D. S. Shekhawat, P. C. Rath, G. K. Joseph and K. Kar, *ACS Nano*, 2019, **13**, 6033-6049.

- 12 L. Adler-Abramovich, L. Vaks, O. Carny, D. Trudler, A. Magno, A. Cafilisch, D. Frenkel and E. Gazit, *Nat. Chem. Bio.*, 2012, **8**, 701.
- 13 W.-P. Hsu, K.-K. Koo and A. S. Myerson, *Chem. Eng. Commun.*, 2002, **189**, 1079-1090.
- 14 K. P. Nartowski, S. M. Ramalheite, P. C. Martin, J. S. Foster, M. Heinrich, M. D. Eddleston, H. R. Green, G. M. Day, Y. Z. Khimyak and G. O. Lloyd, *Cryst. Growth Des.*, 2017, **17**, 4100-4109.
- 15 J. Zhou, X. Du, Y. Gao, J. Shi and B. Xu, *J. Am. Chem. Soc.*, 2014, **136**, 2970-2973.
- 16 N. Zanna, A. Merlettini and C. Tomasini, *Org. Chem. Front.*, 2016, **3**, 1699-1704.
- 17 W. Liyanage, W. W. Brennessel and B. L. Nilsson, *Langmuir*, 2015, **31**, 9933-9942.
- 18 A. Pizzi, L. Lascialfari, N. Demitri, A. Bertolani, D. Maiolo, E. Carretti and P. Metrangolo, *CrystEngComm*, 2017, **19**, 1870-1874.
- 19 D. M. Ryan, S. B. Anderson, F. T. Senguen, R. E. Youngman and B. L. Nilsson, *Soft Matter*, 2010, **6**, 475-479.
- 20 D. M. Ryan, S. B. Anderson and B. L. Nilsson, *Soft Matter*, 2010, **6**, 3220-3231.
- 21 S. Roy and A. Banerjee, *Soft Matter*, 2011, **7**, 5300-5308.
- 22 D. J. Adams, M. F. Butler, W. J. Frith, M. Kirkland, L. Mullen and P. Sanderson, *Soft Matter*, 2009, **5**, 1856-1862.
- 23 A. Bertolani, L. Pirrie, L. Stefan, N. Houbenov, J. S. Haataja, L. Catalano, G. Terraneo, G. Giancane, L. Valli, R. Milani, O. Ikkala, G. Resnati and P. Metrangolo, *Nat. Commun.*, 2015, **6**, 7574.
- 24 A. Pizzi, C. Pigliacelli, A. Gori, Nonappa, O. Ikkala, N. Demitri, G. Terraneo, V. Castelletto, I. W. Hamley, F. Baldelli Bombelli and P. Metrangolo, *Nanoscale*, 2017, **9**, 9805-9810.
- 25 S. M. Ramalheite, J. S. Foster, H. R. Green, K. P. Nartowski, M. Heinrich, P. C. Martin, Y. Z. Khimyak and G. O. Lloyd, *Faraday Discuss.*, 2017, **203**, 423-439.
- 26 L. Arnedo-Sánchez, Nonappa, S. Bhowmik, S. Hietala, R. Puttreddy, M. Lahtinen, L. De Cola and K. Rissanen, *Dalton Trans.*, 2017, **46**, 7309-7316.
- 27 P. Singh, S. Misra, A. Das, S. Roy, P. Datta, G. Bhattacharjee, B. Satpati and J. Nanda, *ACS Appl. Bio Mater.*, 2019, **2**, 4881-4891.
- 28 F. Bergel and J. A. Stock, *J. Chem. Soc.*, 1954, 2409-2417.
- 29 J. L. Andrews, E. Pearson, D. S. Yufit, J. W. Steed and K. Edkins, *Cryst. Growth Des.*, 2018, **18**, 7690-7700.
- 30 C. D. Jones, H. T. D. Simmons, K. E. Horner, K. Liu, R. L. Thompson and J. W. Steed, *Nat. Chem.*, 2019, **11**, 375-381.
- 31 K. Hawkins, A. Patterson, P. A. Clarke and D. K. Smith, *J. Am. Chem. Soc.*, 2020, **142**, 4379-4389.
- 32 J. Ruiz-Olles, P. Slavik, N. K. Whitelaw and D. K. Smith, *Angew. Chem. Int. Ed.*, 2019, **58**, 4173-4178.
- 33 G. R. Krishna, R. Devarapalli, G. Lal and C. M. Reddy, *J. Am. Chem. Soc.*, 2016, **138**, 13561-13567.
- 34 M. Tena-Solsona, J. Nanda, S. Diaz-Oltra, A. Chotera, G. Ashkenasy and B. Escuder, *Chem.-Eur. J.*, 2016, **22**, 6687-6694.
- 35 R. Tatikonda, E. Bulatov, Z. Özdemir, Nonappa and M. Haukka, *Soft Matter*, 2019, **15**, 442-451.
- 36 J. Lerner Yardeni, M. Amit, G. Ashkenasy and N. Ashkenasy, *Nanoscale*, 2016, **8**, 2358-2366.
- 37 L. Meazza, J. A. Foster, K. Fucke, P. Metrangolo, G. Resnati and J. W. Steed, *Nat. Chem.*, 2013, **5**, 42-47.
- 38 K. A. Houton, K. L. Morris, L. Chen, M. Schmidtman, J. T. A. Jones, L. C. Serpell, G. O. Lloyd and D. J. Adams, *Langmuir*, 2012, **28**, 9797-9806.
- 39 M. D. Segarra-Maset, V. J. Nebot, J. F. Miravet and B. Escuder, *Chem. Soc. Rev.*, 2013, **42**, 7086-7098.
- 40 M. Tena-Solsona, S. Alonso-de Castro, J. F. Miravet and B. Escuder, *J. Mater. Chem. B*, 2014, **2**, 6192-6197.
- 41 S. Panja and D. J. Adams, *Chem. Commun.*, 2019, **55**, 10154-10157. View Article Online
DOI: 10.1039/D0SM00584C
- 42 S. Biswas, D. B. Rasale and A. K. Das, *RSC Adv.*, 2016, **6**, 54793-54800.
- 43 E. C. Barker, A. D. Martin, C. J. Garvey, C. Y. Goh, F. Jones, M. Mocerino, B. W. Skelton, M. I. Ogden and T. Becker, *Soft Matter*, 2017, **13**, 1006-1011.
- 44 Y. Lan, M. Lv, S. Guo, P. Nasr, V. Ladizhansky, R. Vaz, M. G. Corradini, T. Hou, S. M. Ghazani, A. Marnangoni and M. A. Rogers, *Soft Matter*, 2019, **15**, 9205-9214.
- 45 C. Tomasini and N. Castellucci, *Chem. Soc. Rev.*, 2013, **42**, 156-172.
- 46 G. Palui, J. Nanda, S. Ray and A. Banerjee, *Chem. – Euro. J.*, 2009, **15**, 6902-6909.
- 47 I. Maity, T. K. Mukherjee and A. K. Das, *New J. Chem.*, 2014, **38**, 376-385.
- 48 S.-M. Hsu, F.-Y. Wu, H. Cheng, Y.-T. Huang, Y.-R. Hsieh, D. T.-H. Tseng, M.-Y. Yeh, S.-C. Hung and H.-C. Lin, *Adv. Healthc. Mater.*, 2016, **5**, 2406-2412.
- 49 Y. Lan, M. G. Corradini, R. G. Weiss, S. R. Raghavan and M. A. Rogers, *Chem. Soc. Rev.*, 2015, **44**, 6035-6058.
- 50 T. Yuan, Y. Xu, C. Zhu, Z. Jiang, H.-J. Sue, L. Fang and M. A. Olson, *Chem. Mater.*, 2017, **29**, 9937-9945.
- 51 S. Basak, S. Bhattacharya, A. Datta and A. Banerjee, *Chem. – Euro. J.*, 2014, **20**, 5721-5726.
- 52 A. Das and S. Ghosh, *Angew. Chem. Int. Ed.*, 2014, **53**, 2038-2054.
- 53 M. R. Molla, A. Das and S. Ghosh, *Chem. – Euro. J.*, 2010, **16**, 10084-10093.
- 54 S. Basak, J. Nanda and A. Banerjee, *J. Mater. Chem.*, 2012, **22**, 11658-11664.
- 55 J. Nanda, A. Biswas and A. Banerjee, *Soft Matter*, 2013, **9**, 4198-4208.
- 56 J. Nanda, A. Biswas, B. Adhikari and A. Banerjee, *Angew. Chem. Int. Ed.*, 2013, **52**, 5041-5045.
- 57 M. A. Spackman and D. Jayatilaka, *CrystEngComm*, 2009, **11**, 19-32.
- 58 M. A. Spackman and P. G. Byrom, *Chem. Phys. Lett.*, 1997, **267**, 215-220.
- 59 E. Mossou, S. C. M. Teixeira, E. P. Mitchell, S. A. Mason, L. Adler-Abramovich, E. Gazit and V. T. Forsyth, *Acta Cryst. C.*, 2014, **70**, 326-331.
- 60 V. K. Aswal and P. S. Goyal, *Curr. Sci.*, 2000, **79**, 947-953.
- 61 J.-Q. Liu, C. Qian, X.-Z. Chen, *Synthesis*, 2010, 403-406.

Table of Contents



Incorporation of nitro ($-\text{NO}_2$) group in phenylalanine makes it an efficient gelator than the native amino acid. The self-assembly and photophysical properties of 4-nitrophenylalanine (4NP) are changed with the alteration of solvent and final self-assembly state of 4NP in competitive solvent mixture are dictated by solvent ratio.